Front. Chem. China 2011, 6(3): 159–163
DOI 10.1007/s11458-011-0248-3

RESEARCH ARTICLE

Mechanical behavior and wrinkling patterns of phase-separated binary polymer blend film

Xuezhe ZHAO, Shengwei DENG, Yongmin HUANG, Honglai LIU (✉) and Ying HU

The wrinkling of phase-separated binary polymer blend film was studied through combining the Monte Carlo (MC) simulation for morphologies with the lattice spring model (LSM) for mechanical properties. The information of morphology and structure obtained by use of MC simulation is input to the LSM composed of a three-dimensional network of springs, which allows us to determine the wrinkling and the mechanical properties of polymer blend film, such as strain, stress, and Young's modulus. The simulated results show that the wrinkling of phase-separated binary polymer blend film is related not only to the structure of morphology, but also to the disparity in elastic moduli between polymers of blend. Our simulation results provide fundamental insight into the relationship between morphology, wrinkling, and mechanical properties for phase-separated polymer blend films and can yield guidelines for formulating blends with the desired mechanical behavior. The wrinkling results also reveal that the stretching of the phase-separated film can form the micro-template, which has a wide application prospect.

Keywords polymer blend film, phase separation, mechanical property, wrinkling, lattice spring model

1 Introduction

Wrinkling of phase-separated polymer blend film is a useful mechanical character for the development and application of new membrane materials. Several wrinkling-based techniques have been applied to measure the elastic modulus of thin film [1–4]. These techniques may serve as the approach to estimate the mechanical properties of thin film such as stability and mechanical performance. Furthermore, these methods ensure a rapid and intrinsically local measurement. For this reason, the application of wrinkling has been a subject of interest..

Another interesting aspect of using the wrinkle is to create film patterns with the specific functions. Bowden et al. reported the reversibility of buckling by cycling between thermal heating and cooling [5]. The study of Chiche et al. shows that the checkerboard patterns are formed by re-stretching a buckled sample perpendicular to the initial stretching direction [6]. Rogers and his coworkers proposed the method based on the buckling-assisted stretchable thin film transistors made of inorganic semiconductors [7,8]. This study can be applied to a route to electronics (and optoelectronics) with extremely high levels of stretchability, compressibility and bendability. However, the reversibility of buckling intending to maintain wrinkling is a fundamental character to fabricate various film patterns.

The coating of failure surface and fabrication of thin film by using spin-coating have been studied with the geometrical configuration of wrinkles [9,10]. Tyagi et al. studied the healing surface defect through computer simulation [11]. It is shown that the application of nanocomposite coating for the notch tip of substrate could potentially yield defect-free surface with enhanced mechanical properties. Researches mentioned above show that control over buckling and analysis of wrinkles are important for nearly all applications of new membrane materials.

Blending of existing polymers is an effective and relatively inexpensive way to create new structural membrane materials. Researchers can tailor the blend to possess the desirable properties of the individual components. Besides, novel structures can be found via wrinkling of this kind of membrane. Recently, many work has focused on the buckling of homogeneous or filled materials, and the research of heterogeneous materials is rare, especially for the phase-separated system.

In this work, we reported the wrinkles and the mechanical behaviors of phase-separated polymer blend films elongated by stretching, by coupling the MC simulation of morphology with the LSM of micro mechanics of materials.

2 Model and method

To determine the micro-phase structure of A/B polymer blend film, first, we adopt the MC simulation on simple cubic lattice based on the bond fluctuation and cavity diffusion algorithms [12–15] with an NVT ensemble. The polymer blend film with

Received June 21, 2011; accepted July 26, 2011
State Key Laboratory of Chemical Engineering and Department of Chemistry, East China University of Science and Technology, Shanghai 200237, China
E-mail: hlliu@ecust.edu.cn

a size of 66 × 66 × 10 is used in simulations. In x and y directions parallel to the film surface, periodic boundary conditions are employed, whereas in z direction perpendicular to the film surface, two impenetrable surfaces are located at $z = 0$ and $z = L_z + 1$. The chain lengths of Polymer A and Polymer B are set equal to 20 and 10, respectively. The repulsive interaction energy between different segments, $E_{A\text{-}B}$, is taken as 0.5 kT and the interaction energies between two identical segments are ignored, i.e., $E_{A\text{-}A} = E_{B\text{-}B} = 0$.

To simulate the wrinkling and mechanical properties of phase-separated binary polymer blend, the three-dimensional Born LSM proposed by Boxton et al. [16] are adopted. Born LSM is a numerical technique of discretizing linear elasticity theory and consists of a network of springs which represent the nearest and next nearest neighboring bonds of a simple cubic lattice. In Born LSM, the harmonic form of elastic energy results in a linear force between neighboring nodes. The constraint that all these linear forces must balance at each node at equilibrium results in a set of linear equation because of the absence of body forces at equilibrium.

$$F_m^{\text{cell}} = -\sum_{n=1}^{N_{\text{cell}}} M_{mn} \cdot \left(\frac{X_{mn} \cdot x_{mn}}{||X_{mn}||} - ||X_{mn}|| \right) \cdot \frac{X_{mn}}{||X_{mn}||} = 0 \quad (1)$$

where N_{cell} is the total number of springs in a cell and Σ_n represents a sum over the nearest- and next-nearest-neighboring nodes. For the node m, $X_{mn} = X_m - X_n$ (X_m is the initial position vector) , $x_{mn} = x_m - x_n$ (x_m is the equilibrium position vector) and M_{nm} is an element of a symmetric matrix **M**, which describes the interaction between nodes m and n through central and noncentral force constants. Eq. (1) represents a set of sparse linear equations. The solution of them is obtained by using a conjugate gradient method to find the equilibrium configuration corresponding to no net force at each node. The central force constant k and noncentral force constant c take the following forms,

$$k = \frac{c}{5(1+2\nu)}$$

$$c = \frac{E(1+4\nu)}{5(1-\nu)(1+2\nu)} \quad (2)$$

where E and v are the Young's modulus and Poisson's ratio, respectively [16–18].

At the beginning of simulation, the local force constants are specified at nodal points straddling the boundary between two phases or two nodes according to a series of spring systems weighted by the partial lengths. A force constant k_{mn} between nodes m and n is defined as

$$k_{mn} = \frac{l k_{mm} \cdot k_{nn}}{l_n k_{mm} + l_m k_{nn}} \quad (3)$$

where l_m and l_n represent the partial lengths of the spring that belong to the respective domains, and $l = l_m + l_n$ [19,20].

3 Results and discussion

We focus on the influence of the composition of polymer blend on the morphology and mechanical property of polymer blend. The volume fraction of polymer A, f_A, is varied from 0.1 to 0.9. The result of simulation shows that the morphology of A/B polymer blend film is strongly dependent on the composition of the polymer blend.

It is observed that when f_A increases from 0.1 to 0.5, the cylindrical polymer A phase is surrounded by the continuous skeleton of B phase, and the size of the cylindrical polymer A domain increases with the increase of f_A. When f_A increases to 0.6 or further, the polymer B phase is surrounded by a continuous skeleton of A phase, the polymer A phase becomes continuous and the polymer B phase becomes the cylindrical phase with regular size.

To investigate the mechanical behavior in the direction parallel to the film surface, we deform the systems through the application of a strain at the system boundaries.

For convenience, besides specially assigned, Young's modulus of the pure polymer A and the pure polymer B are taken as 2.965×10^3 MPa and 0.942×10^3 MPa, respectively. Poisson's ratios of the polymer A and B are set as 0.360 and 0.420, respectively. This represents a different elastic disparity for polymeric systems, such as difference between polystyrene (PS) and polypropylene (PP). The system is equilibrated at a global deformation that corresponds to a strain of 4%. In this study, the cavities distributed in film are neglected and all results are depicted through triple expansion.

When a force is applied in the x direction parallel to the film surface, the linear elastic system is strained in the x direction. The springs that possess a component in the x direction are more extended than springs that are oriented normally to the x direction. The interfacial boundaries between two phases or two nodes are assigned intermediate spring constants through a simple linear rule of mixture, such as Eq. (3). This disparity in elastic moduli results in complex elastic fields, which leads to an interesting mechanical behavior of the thin film of polymer blend related with morphologies. The tensile deformation in the x direction is applied to the samples with different morphologies. The variation of volume fraction results in different micro-structures, and these structures directly influence the wrinkle and the distribution of strain and stress.

For convenience, we first study the distribution of strain and stress of the film surface.

Figure 1 depicts the variation field of the normal strain ε_{xx}

and the stress σ_{xx} for morphology with $f_A = 0.3$. In this case, the strain and stress are rescaled to the value between 0 and 1, and the lighter regions correspond to higher strains and stresses. From Fig. 1, it is obvious that the strain and stress field match with the morphologies of polymer blends nearly perfect, indicating that the strain field and stress field are directly influenced by the morphology with the elastic constants used in LSM. Fig. 1 shows the strain field and stress field in a system where the minority phase (A phase) is stiffer than the majority phase (B phase), and therefore, the strain field (Fig. 1b) is concentrated on the majority phase. These strain concentrations are the greatest on the regions with the shortest distance between the boundaries of the minority stiffer phases, which are parallel to the direction of the applied strain. In particular, when the minority stiffer phases have small sizes, there are maximum strain concentrations in the boundaries of the minority stiffer phases. The stress field (Fig. 1c) concentrations extend from the minority stiffer phases through the boundaries of these phases (along the direction parallel to the applied strain).

Figure 2 shows the strain field and stress field in a system where the majority phase (A phase) is stiffer than the minority phase (B phase). As shown in Fig. 2b, the strain field is concentrated in the minority softer phase. The regions of the maximum strain are almost within the minority softer phase. The regions of the minimum strain are exclusively within the regions with the shortest distance between the boundaries of the minority softer phases, which are parallel to the direction of the applied strain. In Fig. 2c, the stress field is concentrated in the region of majority stiffer phase (along the direction perpendicular to the applied strain). The regions of the minimum stress are almost within the minority softer phase and extend from the minority softer phases through the boundaries of the minority softer phases (along the direction parallel to the applied strain). The results of the above simulation show that the local mechanical response is affected by altering the relative ratio and type of morphology of the stiffer and softer components. The enhanced strain and stress concentrations are responsible for the onset of crack propagation and the premature failure of the entire system. We can also research the wrinkling of the film on the basis of the analysis of the strain and stress field. The wrinkling of the polymer blend film is worthy of attention for the study of mechanical properties of film surface, such as surface fracture, coating and painting. We depict such a layer of film only for the convenience of visual judgment. Moreover, the height of wrinkling is rescaled to the value between 0 and 1. The results of simulation show that the wrinkling of the surface of polymer blend film is closely related to its strain and stress field.

Figure 3a shows that the surface wrinkling matches to its strain, although there is a contrarotation of height. It shows that the minority stiffer phases have the maximum height of wrinkle. The minimum height of wrinkle is found in the region with the shortest distance between the boundaries of minority stiffer phases (along the direction parallel to the applied strain). Fig. 3b depicts that the type of wrinkling is typically similar to its strain field with the contrarotation of height.

The maximum height of wrinkle is within the region of majority stiffer phases with the shortest distance between the boundaries of minority softer phases (along the direction parallel to the applied strain). The low height of wrinkle are found in the regions of minority softer phases. However, both Fig. 3a and 3b show that the regions with high height of wrinkle are within the regions of stiffer phases.

Our simulation results show that the wrinkling of porous film obtained via the removal of minority phases is similar to the wrinkling of Fig. 3b, whether the minority phases are stiffer than the majority phases or not. Fig. 4 depicts the wrinkling of porous films obtained from binary polymer blends with volume fraction $f_A = 0.3$ (a) and $f_A = 0.7$ (b). These results provide useful information for the fabrication and the application of porous film such as molecular sieve and artificial biofilm.

Through the simulation of the wrinkles, we can evaluate

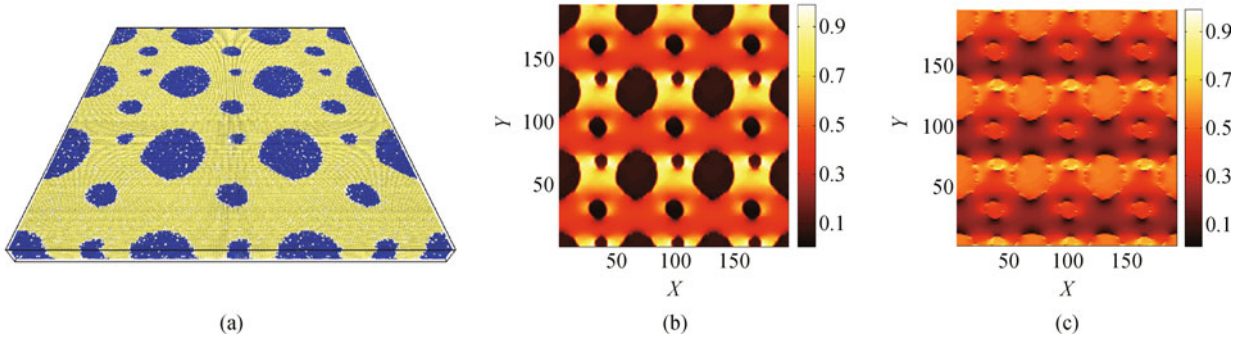

Figure 1 Morphology (a), normal strain (b) and stress (c) field (at the surface $z = 10$) for the film with $f_A = 0.3$

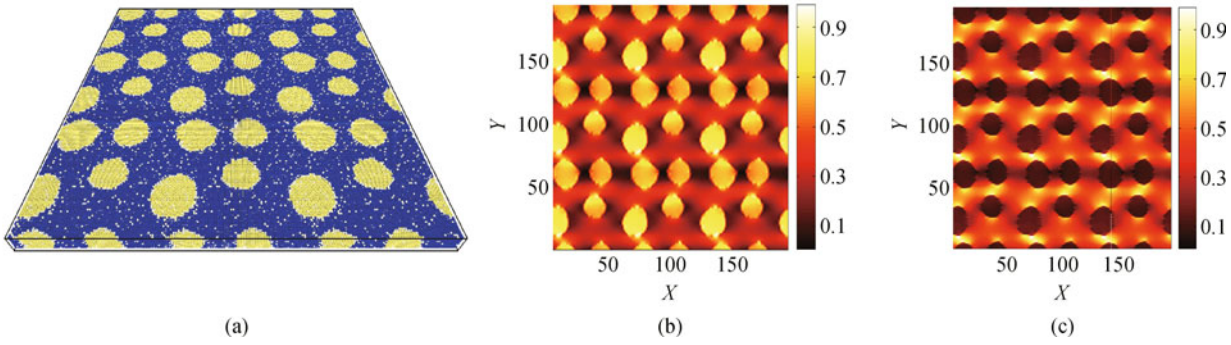

Figure 2 Morphology (a), normal strain (b) and stress (c) field (at the surface z = 10) for the film with f_A = 0.7

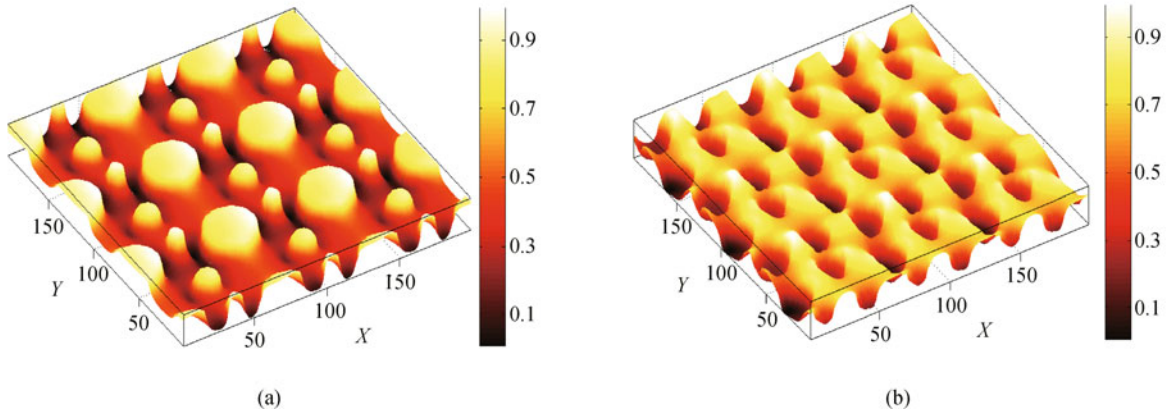

Figure 3 The wrinkling of surfaces of polymer blend film with f_A = 0.3 (a) and f_A = 0.7 (b)

visually the mechanical behavior of the heterogeneous film system such as surface coating and fracture.

4 Summary and conclusions

The two computational models (MC and LSM) are coupled in such a method as to determine the wrinkling and mechanical properties of phase-separated binary polymer blend film. Our simulation results show that the wrinkling of the surface of polymer blend film is closely matched with its strain and stress field related to the volume fraction and the disparity in elastic moduli.

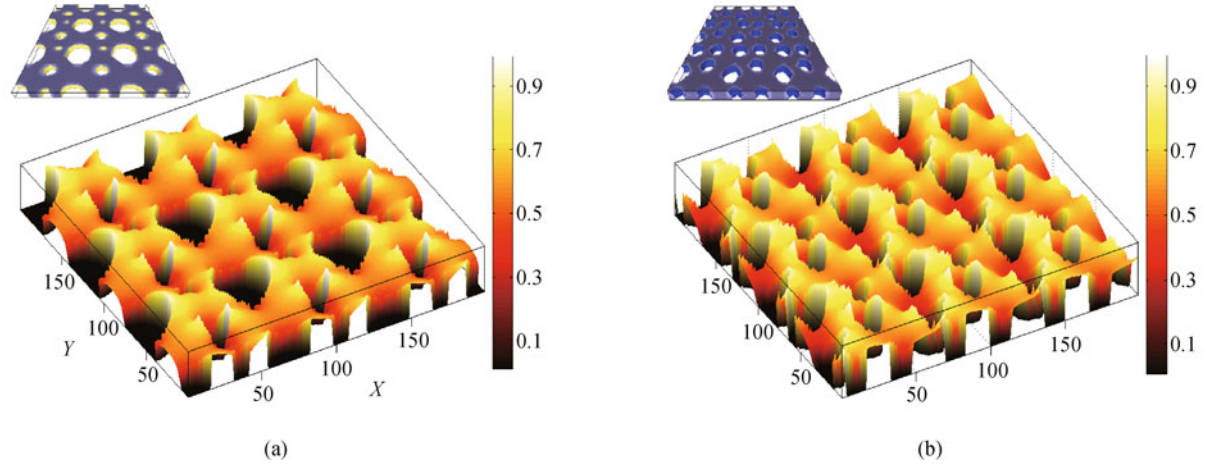

Figure 4 The wrinkling of surfaces of porous films obtained by removal of minority phases in the films with f_A= 0.3 (a) and f_A= 0.7 (b)

Our simulation method and results could be served not only to analyse the wrinkle, strain and stress of phase-separated polymer blend film, but also to predict the mechanical properties such as Young's modulus. The increase of film thickness results in more varied structures such as sphere, straight band and straight band incorporated with sphere, except for single cylinder, although these results have not been presented in this paper. These results would permit to enlarge its application. Moreover, a control over the composition of blends, stretching direction of film and the filling of the third ingredient enable us to design the functional film with various structures because of the morphological diversity of phase-separated polymer blend film.

Acknowledgements Financial support for this work was provided by the National Natural Science Foundation of China (Nos. 20976044, 20736002), Program for Changjiang Scholars and Innovative Research Team in University of China (Grant No. IRT0721) and the 111 Project of China (Grant No. B08021).

References

1. Stafford, C. M.; Harrison, C.; Beers, K. L.; Karim, A.; Amis, E. J.; VanLandingham, M. R.; Kim, H. C.; Volksen, W.; Miller, R. D.; Simonyi, E. E., *Nat. Mater*. **2004**, *3*, 545–550
2. Huang, J.; Juszkiewicz, M.; de Jeu, W. H.; Cerda, E.; Emrick, T.; Menon, N.; Russell, T. P., *Science* **2007**, *317*, 650–653
3. Nolte, A. J.; Cohen, R. E.; Rubner, M. F., *Macromolecules* **2006**, *39*, 4841–4847
4. Aamer, K. A.; Stafford, C. M.; Richter, L. J.; Kohn, J.; Becker, M. L., *Macromolecules* **2009**, *42*, 1212–1218
5. Bowden, N.; Brittain, S.; Evans, A. G.; Hutchinson, J. W.; Whitesides, G. M., *Nature* **1998**, *393*, 146–149
6. Chiche, A.; Stafford, C. M.; Cabral, J. T., *Soft Matter* **2008**, *4*, 2360–2364
7. Sun, Y.; Choi, W. M.; Jiang, H.; Huang, Y. Y.; Rogers, J. A., *Nat. Nanotechnol*. **2006**, *1*, 201–207
8. Khang, D. Y.; Jiang, H.; Huang, Y.; Rogers, J. A., *Science* **2006**, *311*, 208–212
9. Hayward, R. C.; Chmelka, B. F.; Kramer, E. J., *Macromolecules* **2005**, *38*, 7768–7783
10. Singamaneni, S.; Tsukruk, V. V., *Soft Matter* **2010**, *6*, 5681
11. Tyagi, S.; Lee, J. Y.; Buxton, G. A.; Balazs, A. C., *Macromolecules* **2004**, *37*, 9160–9168
12. Reiter, J.; Edling, T.; Pakula, T., *J. Chem. Phys*. **1990**, *93*, 837–844
13. Carmesin, I.; Kremer, K., *Macromolecules* **1988**, *21*, 2819–2823
14. Larson, R. G.; Scriven, L. E.; Davis, H. T. J., *Chem. Phys*. **1985**, *83*, 2411–2420
15. Larson, R. G., *J. Chem. Phys*. **1989**, *91*, 2479–2488
16. Buxton, G. A.; Care, C. M.; Cleaver, D. J., *Model. Simul. Mater. Sci. Eng*. **2001**, *9*, 485–497
17. Buxton, G. A.; Balazs, A. C., *Macromolecules* **2005**, *38*, 488–500
18. Shou, Z.; Buxton, G. A.; Balazs, A. C., *Compos. Interfaces* **2003**, *10*, 343–368
19. Buxton, G. A.; Balazs, A. C., *Mol. Simul*. **2004**, *30*, 249–257
20. Ostoja-Starzewski, M.; Sheng, P. Y.; Jasuik, I., *Eng. Fract. Mech*. **1997**, *58*, 581–606